Heavy Ion Flows in the Upper Ionosphere of the Venusian North Pole

M. Persson, Y. Futaana, H. Nilsson, G. Stenberg Wieser, M. Hamrin, A. Fedorov, T. L. Zhang, S. Barabash

AGU100 ADVANCING EARTH AND SPACE SCIENCE

JGR Space Physics

RESEARCH ARTICLE
10.1029/2018JA026271

Heavy Ion Flows in the Upper Ionosphere of the Venusian North Pole

M. Persson[1], Y. Futaana[1], H. Nilsson[1], G. Stenberg Wieser[1], M. Hamrin[2], A. Fedorov[3], T. L. Zhang[4], and S. Barabash[1]

[1]Swedish Institute of Space Physics, Kiruna, Sweden, [2]Department of Physics, Umeå University, Umeå, Sweden, [3]IRAP, CNRS, Toulouse, France, [4]Space Research Institute, Austrian Academy of Sciences, Graz, Austria

Key Points:
- A net dusk-to-dawn heavy ion flow across the polar region was found, with high speeds inside the collisional region of the ionosphere
- The heavy ion flow pattern does not depend on the external interplanetary field directions or the magnetization state of the upper ionosphere
- We suggest a thermal pressure gradient between the polar and equatorial terminator regions as an accelerating mechanism toward the pole

Supporting Information:
- Supporting Information S1

Correspondence to:
M. Persson,
moa.persson@irf.se

Citation:
Persson, M., Futaana, Y., Nilsson, H., Stenberg Wieser, G., Hamrin, M., Fedorov, A., et al. (2019). Heavy ion flows in the upper ionosphere of the Venusian North Pole. *Journal of Geophysical Research: Space Physics*, *124*, 4597–4607. https://doi.org/10.1029/2018JA026271

Received 19 NOV 2018
Accepted 3 MAY 2019
Accepted article online 9 MAY 2019
Published online 13 JUN 2019

Abstract We investigate the heavy ion density and velocity in the Venusian upper ionosphere near the North Pole, using the Ion Mass Analyzer, a part of the Analyzer of Space Plasmas and Energetic Atoms 4, together with the magnetic field instruments on Venus Express. The measurements were made during June–July 2014, covering the aerobraking campaign with lowered altitude measurements (~130 km). The plasma scale heights are ~15 km below 150-km altitude and ~200 km at 150–400-km altitude. A clear trend of dusk-to-dawn heavy ion flow across the polar ionosphere was found, with speeds of ~2–10 km/s. In addition, the flow has a significant downward radial velocity component. The flow pattern does not depend on the interplanetary magnetic field directions nor the ionospheric magnetization states. Instead, we suggest a thermal pressure gradient between the equatorial and polar terminator regions, induced by the decrease in density between the regions, as the dominant mechanism driving the ion flow.

Plain Language Summary We have calculated the ion density and velocities in the Venusian polar ionosphere using measurements from the Ion Mass Analyzer on board the Venus Express spacecraft. During June–July 2014 the periapsis was lowered to ~130 km, which allowed for measurements down to low altitudes of the ionosphere near the North Pole. The plasma scale heights are ~15 km below 150-km altitude and ~200 km at 150–400 km, which is similar to what was found near the equatorial region by the Pioneer Venus mission. In addition, there is a clear trend of dusk-to-dawn flow, along the terminator, for the heavy ions. This is surprising, as a general flow from day-to-night is expected for the Venusian ionosphere due to the long nights and significant heating of the dayside upper atmosphere. The interplanetary magnetic field direction does not appear to affect the ion flow pattern. Instead, we propose a thermal pressure gradient as the dominant accelerating mechanism, induced by the decrease in density from the equator toward the pole.

1. Introduction

Venus, in contrast with Earth, does not possess an intrinsic magnetic field. Due to its proximity to the Sun, Venus has a large ionization rate and heating in the dayside upper atmosphere. The ionization creates an extensive conductive ionosphere on the dayside. The incoming interplanetary magnetic field (IMF) induces currents in the conductive ionosphere diamagnetically. The induced magnetic field is capable of withstanding the solar wind pressure. The produced void is called an induced magnetosphere (see review by Futaana et al., 2017, and references therein). On the other hand, measurements on the nightside ionosphere (e.g., Mariner Stanford Group, 1967) showed that the ion density on the nightside is higher than expected. In the nightside ionosphere, no ionization by solar radiation is possible, so that the plasma cannot be explained only by the atmospheric superrotation (four days) due to the short ion lifetime (Butler & Chamberlain, 1976). Rather, the day-night transport of ionospheric plasma may play a key role. The study of the ion dynamics and chemistry is, therefore, essential to understand the Venus ionosphere, and its interaction with the neutral atmosphere on one side and with the solar wind on the other.

Pioneer Venus Orbiter (PVO) studied the Venus ionosphere extensively. During its first three years, PVO made in situ measurements of the Venus ionosphere, down to an altitude of 150 km. PVO had an equatorial orbit, with a drift of the local time of the pericenter due to the rotation of the planet around the Sun (Colin, 1980). The drift made it possible to make low altitude (<200 km) measurements of the Venusian ionosphere in the near-equatorial region over a wide local time range (Taylor et al., 1979). The flow of ions in the equatorial region was studied using the Orbiter Retarding Potential Analyzer instrument on board PVO

(Knudsen et al., 1979). A large horizontal flow of ions across the terminator from the dayside toward the nightside was found with a mean velocity of 2–3 km/s, whereas the flow speed increased with increasing altitude. The ion flux across the terminator maintains the nightside ions, and heats the nightside ionosphere (Knudsen et al., 1980). The large trans-terminator flow was produced mainly by the large pressure gradient between the dayside and nightside ionospheres (Knudsen et al., 1981).

Considering only the pressure gradient between day and night, the ion flow from dayside to nightside should be axisymmetric around the Venus-Sun line. However, Orbiter Retarding Potential Analyzer measurements showed that this is not entirely true (Knudsen et al., 1980). There is an asymmetry between the dawn and dusk region both in the ion density and flow. The ion flow velocities are larger on the duskside than on the dawnside and the ion density is slightly lower on the dawnside than on the duskside. This asymmetry could be explained by introducing a retrograde superrotation of 400 m/s of the upper atmosphere and ionosphere, both for the ion density (Miller et al., 1984) and the ion flow below 400 km. The superrotation speed of the ionosphere is therefore much larger than that found for the neutral atmosphere at ~100 m/s. Above 400 km, however, the superrotation of the ionosphere was found to be prograde (Miller & Knudsen, 1987).

The recent Venus Express (VEx) mission probed the upper ionosphere of Venus near the North Pole during the Atmospheric Drag Experiment campaigns. During the 12 campaigns between 2008 and 2013 the pericenter altitude of VEx was lowered down to 160 km for several consecutive orbits. These campaigns were designed primarily to make in situ measurements and allow us to characterize the neutral atmospheric density profile and investigate the thermosphere dynamics (e.g., Bougher et al., 2006; Müller-Wodarg et al., 2006). To measure the total neutral density in the altitude range 160–200 km the solar arrays were placed in an asymmetric position during the Venus Express Atmospheric Drag Experiment campaigns. The total torque acting on the spacecraft, due to the asymmetric configuration, was measured and counteracted by the attitude control system. From the total measured torque, the total neutral density was calculated, combined with the spacecraft body and solar array configurations (Limaye et al., 2017). The measurements showed a lower density by 1 order of magnitude in the polar region, within the altitude range of 160–200 km, compared to the density measured in the equatorial terminator region (Limaye et al., 2017).

Ion measurements from the Analyzer of Space Plasmas and Energetic Atoms (ASPERA-4) instrument on board VEx showed that the ions and energetic neutral atoms have a strong dusk-to-dawn flow across the pole at altitudes higher than 250 km, in contrast with the measurements of PVO in the equatorial atmosphere. The mass flux of the ionospheric ions was observed to increase below the ionopause, while the solar wind mass flux decreased, which could indicate a transfer of momentum from the solar wind to the ionospheric heavy ions by means of friction between the two plasma populations (Lundin et al., 2011, 2014). Lundin et al. (2014) hypothesized that the dusk-to-dawn flow pattern over the pole is a consequence of the 5° aberration angle of the solar wind from the orbital motion of Venus. The momentum transfer to the ionosphere would happen through wave-particle interactions at the induced magnetosphere boundary, and through Coulomb collisions between the ionospheric ions to the lower altitudes (Perez-de-Tejada et al., 2010). Below 500 km the mass flux of heavy ions starts to decrease significantly, which is suggested to be energy and momentum loss from the ions to the neutrals through ion drag (Lundin et al., 2011).

The ion movements in the Venusian ionosphere are also affected by the presence of the magnetic fields. The Venusian ionosphere can be in either a magnetized or an unmagnetized state (Angsmann et al., 2011; Russell & Vaisberg, 1983; Zhang et al., 2008). When the solar wind dynamic pressure is high, the IMF can enter the ionosphere and add to the internal pressure to keep the pressure balance at the ionopause (Russell & Vaisberg, 1983). This case is called the magnetized state of the ionosphere, and the ionopause in the subsolar region in this state is located at below 300-km altitude. In addition, the magnetic field strength generally decreases with increasing solar zenith angle, and the ionopause is typically located at higher altitudes in the terminator region than in the subsolar point. On the other hand, in the unmagnetized state, there are almost no magnetic fields in the ionosphere, with the exception of small-scale flux ropes. The magnetization can be explained by a diffusion/convection model of the magnetic fields in the ionosphere, where the ions have a vertical downward flow of ~10 m/s that brings the magnetic field down into the lower ionosphere with a characteristic time scale of ~1 hr (Luhmann & Cravens, 1991, and references therein).

The MAG instrument on board VEx measured the magnetic field in the Venus ionosphere (Zhang et al., 2007). Dubinin et al. (2014) found that the magnetic field direction measured in the polar region

(~200 km) in general is in the dusk-dawn direction and is not dependent on the direction of the *y* component of the IMF. Instead, the magnetic field direction is dependent on the ion-electron motion-induced currents in the lower altitudes. Further, the magnetic pileup region was found to be located above 400-km altitude in the polar region and the ionosphere was generally magnetized down to ~200-km altitude (Dubinin et al., 2014).

Between June and July of 2014, VEx pericenter was lowered down to 130 km to conduct aerobraking. The magnetic field measured during these low-altitude passages showed a tendency to decrease in average total strength down to 140 km, below which it was constant. Meanwhile, the variability was observed to further decrease down to the pericenter, showing a very quiet magnetic field below 140 km, at which altitude the ionospheric electron density peak is located. Presumably, below the ionospheric peak no strong currents can be carried, and thus, no current layers are contributing to the magnetic field (Zhang et al., 2016).

In this study, we use the low-altitude measurements during the VEx aerobraking campaign to discuss the heavy ion flow and density distribution in the Venus polar ionosphere. In section 2 we describe the instrument and the method used to calculate the heavy ion velocity and density. We present the results of the measurement in section 3 and our interpretation in section 4. Our conclusions are in section 5.

2. Instrument and Method

This study uses the in situ measurements of ions in the Venus ionosphere made by the Ion Mass Analyzer (IMA) sensor as a part of the ASPERA-4 instrument on board VEx (Barabash et al., 2007). In addition, we used magnetometer data measured by the MAG instrument (Zhang et al., 2007).

VEx conducted its science operation from April 2006 until November 2014, when it ran out of fuel and later incinerated in the Venusian atmosphere in January 2015. VEx had a polar orbit around Venus with a nominal pericenter altitude of typically 250 km close to the North Pole. The apocenter altitude was approximately 66,000 km, which gave the total orbit period of 24 hr (Svedhem et al., 2007). During June to July 2014, VEx went into the aerobraking campaign, where the pericenter altitude was lowered down to ~130 km before raising the pericenter again. In this study, we use ionospheric ion measurements from 64 pericenter passes of VEx from 1 June to 1 August 2014, which covers the aerobraking campaign period.

IMA had 16 azimuthal sectors of 22.5° each and an electrostatic sweep of 16 steps in elevation with 5.6° resolution, which gave a total field of view of $>2\pi$. The instrument was designed to measure ions of energies between 0.01 and 36 keV/q, with a resolution of $\Delta E/E = 7\%$. The primary science objectives, which did not include the lower ionospheric measurements, limited the lowest capable energy to 0.01 keV/q (Barabash et al., 2007). Using a permanent magnet assembly the mass of ions was resolved (M/Q = 1–>40 amu). Over 192 s, IMA provides a 3-D energy spectra of the ions. See Barabash et al. (2007) for more information about the instrument. The main focus in this study lies on the heavy ions (O^+, $O_2{}^+$, and $CO_2{}^+$), with a small contribution on the H^+ and He^+ ions.

IMA data from one pericenter pass obtained on 2 July 2014 are displayed in Figure 1. As seen in Figure 1a, the spacecraft moved from the solar wind across the bow shock at 15:50 and encountered the induced magnetospheric boundary at 16:20. After reaching the pericenter at 16:28 (lowest altitude in Figure 1b, VEX again crossed the induced magnetosphere boundary at 16:37 and moved across the bow shock again at 17:15; Figures 1c and 1d show the 192-s data obtained in the ionosphere (~200 km), and Figures 1e and 1f) show the data in the lower ionosphere (~130 km). The corresponding time periods are specified in Figure 1a.

Figure 1c shows the energy-mass spectrogram. Three main populations can be seen on the curves of $\boldsymbol{M/Q}$ = 1, 4, and 16, where the heavy ions exhibit a wide spread. These three signals can be considered as H^+, He^+, and O^+, although O^+ may be contaminated by $O_2{}^+$ and $CO_2{}^+$ (as for Mars; Carlsson et al., 2006). We assume this component as O^+ because it is the major ion in Venus upper ionosphere (>180 km; e.g., Fox & Sung, 2001; Taylor et al., 1980).

Figure 1d shows the angular distribution of the measured ions in the IMA instrument frame. This measurement was done at ~330 km, but represents a typical measurement of ions in the ionosphere above ~200 km.

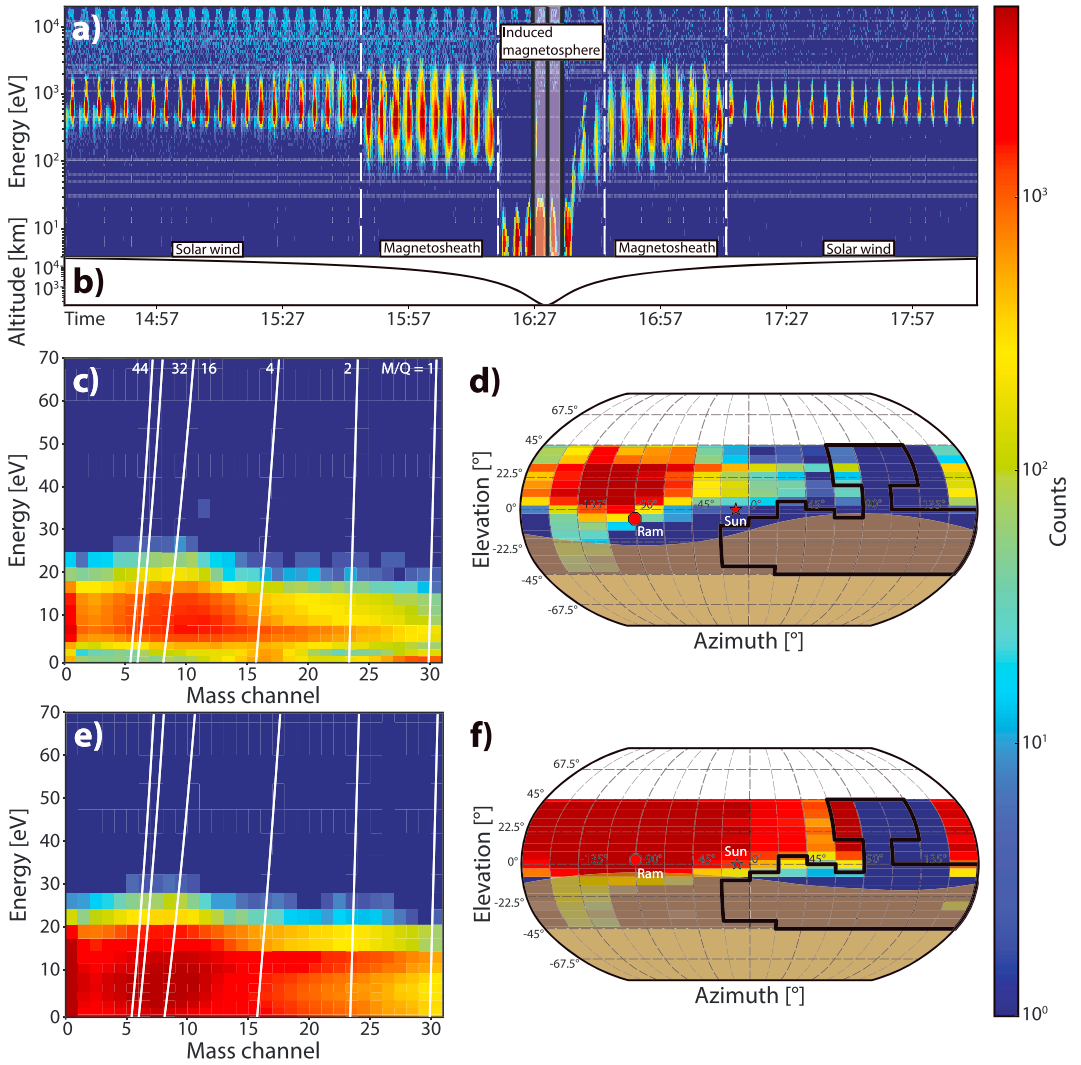

Figure 1. Typical IMA data over one pericenter pass obtained on 2 July 2014. The color scale in each panel corresponds to the number of measured ion counts per pixel. (a) Energy-time spectrogram of ions, that is, energy on vertical axis and time on horizontal axis. The grey areas at 16:27 and 16:30 indicate the 192-s full scan corresponding to the periods shown in (c)–(f). Plasma domains and their boundaries where VEx was located are also indicated. (b) Altitude of VEx. (c) Energy-mass spectrogram of ions at 16:30. The white curves indicate the mass per charge of ions (M/Q = 1, 2, 4, 16, 32, and 44) obtained from ground calibration. (d) Measured arrival direction of heavy ions in the field-of-view projection in the instrument frame at 16:30. The elevation is on the vertical axis and the azimuth on the horizontal axis. The dark yellow area indicates the Venus body, a red star in the center is the Sun direction, and the large red circle is the spacecraft ram direction. The black wire frame shows the maximum blocking direction by the spacecraft body. (e) The pericenter measurement (see text for more details) at 16:27 in the same format as (c). (f) The pericenter measurement at 16:27 in the same format as (d). All the energy information in (a), (c), and (e) was corrected by the empirical method, described in detail in section S1 in the supporting information.

The majority of the flux around the main peak of the distribution is located inside the field of view and is not blocked by the spacecraft body. This means that the IMA measurement could cover the incoming direction of ions almost fully. The main peak is clearly shifted from the spacecraft ram direction, indicating that the ions have a velocity in the ionosphere.

Near the pericenter there are much stronger signals in the measurements (Figures 1e and 1f), with wider spreads in mass, energy, and angular bins. We have separated such data points from the rest in the following analysis, and named them “pericenter measurements,” typically seen below 200 km. We chose to use the full mass channel range of this data, and integrate for one species. Due to the significantly wide spread over the

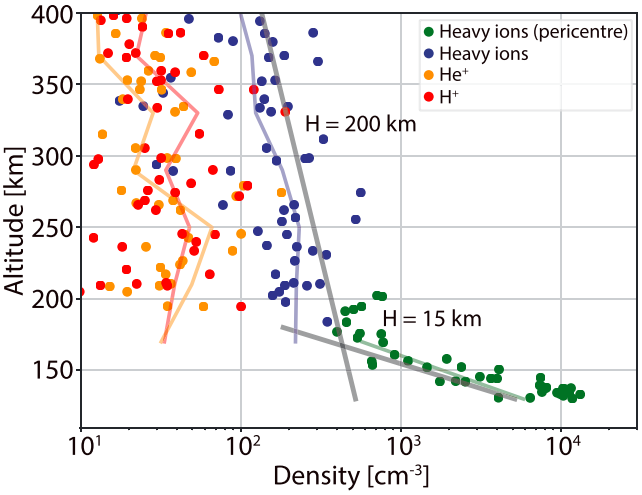

Figure 2. Statistical altitude profile of the ion densities of H^+ (red), He^+ (orange), and heavy ions, both nominal (O^+, blue) and pericenter (O_2^+, green) measurements (see section 2 for details), measured by IMA between 1 June and 1 August 2014. Each data point corresponds to a measurement over 192-s full scan. The mean profiles are shown by solid lines. The straight gray lines indicate the scale heights.

mass channels, the mass could not be discriminated from the measurements; thus, mass 32 (O_2^+) is assumed in the further analysis as the O_2^+ ions were previously found to dominate in this altitude region (<180 km; Fox & Sung, 2001; Taylor et al., 1980) compared to all the other species (H^+, He^+, O^+, etc.). The wider angular distribution of these measurements, spreading beyond the instrument field of view, might lead to a slight underestimation of the density.

The energy scales in Figures 1a, 1c, and 1e have been corrected by removing a plausible instrument effect on the energy scale mainly due to an unknown offset of the high-voltage power supply of the IMA instrument, combined with the unknown spacecraft potential. As the IMA instrument was not optimized to measure the ionospheric ions (i.e., beam-like low-energy ions), an empirical calibration of the energy scale offset is needed. The details of the full offset calculations are included in the supporting information. In summary, the offset of the energy scale was found to be 16.7 eV, which was subtracted from the default energy table of IMA. Note that the offset of 16.7 eV includes the spacecraft potential, which cannot be separated from the offset of the high-voltage power supply in the empirical method used. We have employed an error analysis by varying the offset by ±5 V; the results indicate that the density profile (Figure 2) and flow pattern of the ionospheric ions (Figure 3) did not change much. Therefore, we use the calculated offset in the following discussion. Indeed, with the help of the 16.7-eV offset and the spacecraft motion (7–8 km/s), the IMA instrument could measure the ionospheric ions. The incoming ions were accelerated by the 16.7 eV inside the instrument before reaching the detector, and thus, even the ions stationary in the spacecraft frame would get energies above the IMA's intrinsic lower energy limit (10 eV).

The spacecraft potential may also influence the coming direction of the ions. Due to the accommodation of the instrument with regards to the spacecraft structure, the observed ions would not have deviated much because the incoming directions of the ions and spacecraft structure are separated enough (see more details in section S2 in the supporting information). In addition, to evaluate the influence of the results due to shifts in angular directions, we deviated the bulk velocity vector in the IMA frame by 20°, corresponding to the full width at half maximum of the angular distribution. Propagating this deviation results in ~10° in the resulting vector direction (see section S2 in the supporting information). Hence, we conclude that the shift in ram direction is likely due to the ion velocity in the ionosphere, rather than the spacecraft potential or statistical error.

From each set of full energy and elevation scans of IMA (192-s data), the density and velocity of the heavy ions were derived by calculating plasma moments (Fränz et al., 2006). Thus, each 192-s measurement gives one data point of the ion density as well as the velocity vector. Over the full scan of the IMA instrument, the spacecraft moves ~1,000 km, mainly horizontally, due to the high speed of VEx (~8 km/s). To mitigate the large ambiguity in location, the measurement epoch was assigned as the time when the maximum counts are measured in the 3-D spectrum.

3. Results

Figure 2 shows the obtained altitude profiles of the H^+, He^+, and heavy ion density (O^+ assumed for >~200 km and O_2^+ for <~200 km (pericenter measurements)). All the available data between 1 June and 1 August 2014 are used. From this statistical profile, a general trend of decreasing density with increasing altitude for all three species can be seen. For the heavy ions, the scale height $\boldsymbol{H_p}$ is found as $\boldsymbol{H_p}$~15 km in the altitude range of 130–200 km, where there are mostly pericenter measurements. The scale height becomes $\boldsymbol{H_p}$~200 km above the altitude of 200 km. These scale heights are similar to those measured by PVO in the subsolar region, where the scale height was found to be $\boldsymbol{H_p}$ = 10 km in the altitude range 150–180 km and $\boldsymbol{H_p}$ = 100 km above 180-km altitude (Taylor et al., 1980). The clear change in scale height at 200 km is consistent with modeling results of the Venusian ionosphere (Fox & Sung, 2001). The change in scale height is correlated

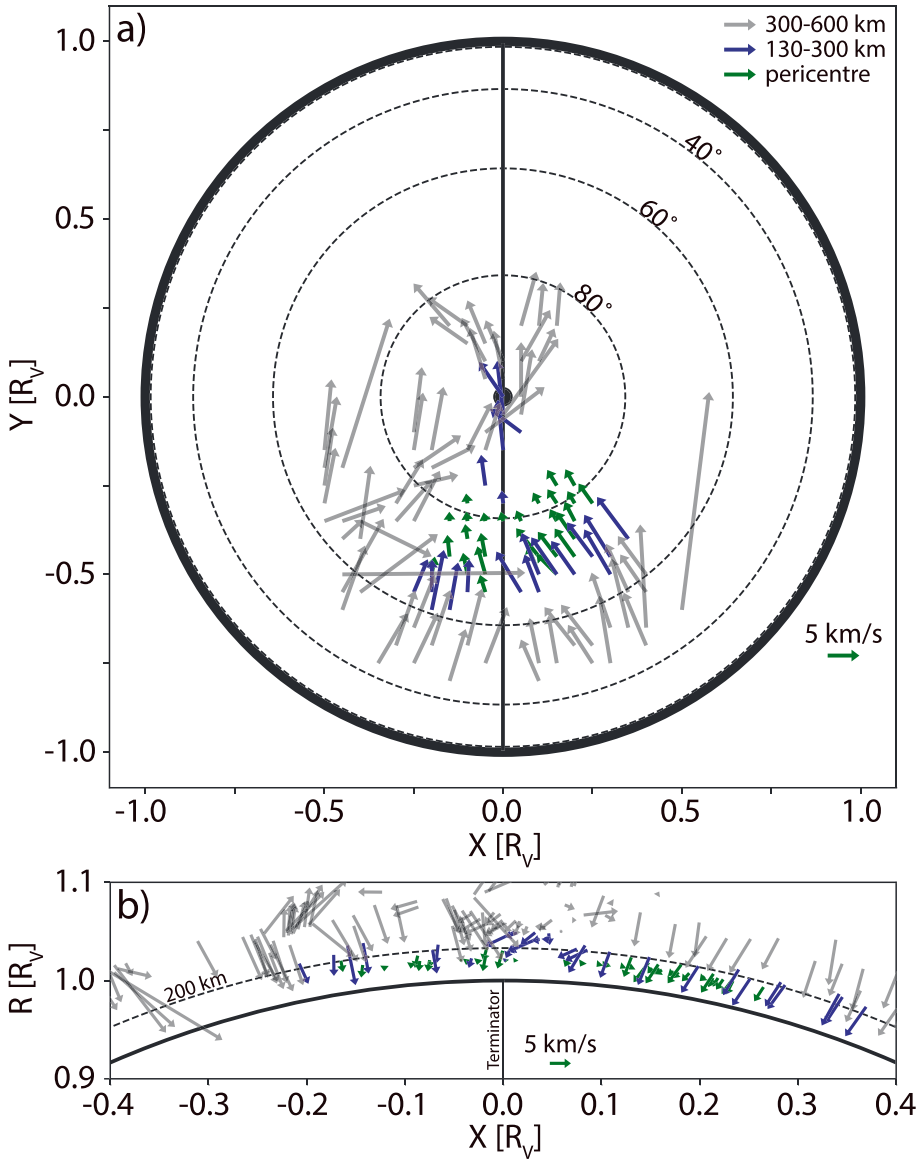

Figure 3. Heavy ion velocity vectors projected in (a) the *X*-*Y* plane and (b) the ***X*-*R*** ($R=\sqrt{Y^2+Z^2}$) plane. The altitudes of the measurement are shown by the colors on the arrows: blue for 180–300 km, grey for 300–600 km, and green for the pericenter measurements (<~180 km). In (a) the North Pole is located in the middle and the dashed circles represent latitudes, with the solid circle showing the outer rim of Venus. In (b) the solid curve represents the Venusian surface and the dashed curve is the altitude of 200 km.

with the change in composition, where in the lower altitude O_2^+ is the major ion and in the higher altitude O^+ is the major ion. The change in ion composition is due to chemical processes between the neutrals and ions, where the major ion shifts from CO_2 to O at ~200 km (Hedin et al., 1983), and the change from mainly a photochemical regime to a diffusion regime above ~200 km (Fox & Sung, 2001).

On the other hand, the absolute value of the density is about 2 orders of magnitude lower than the subsolar ion densities measured by PVO (Taylor et al., 1980). This may be attributed to the fact that the IMA instrument was not designed to measure ionospheric ions, and thus, the absolute density is hardly constrained. Rather, we focus on the relative density profiles (scale height) in this altitude range.

The ion temperatures of the measured heavy ions may be calculated from the scale heights. In a diffusive equilibrium region the plasma scale height $\boldsymbol{H_p}$ is given by

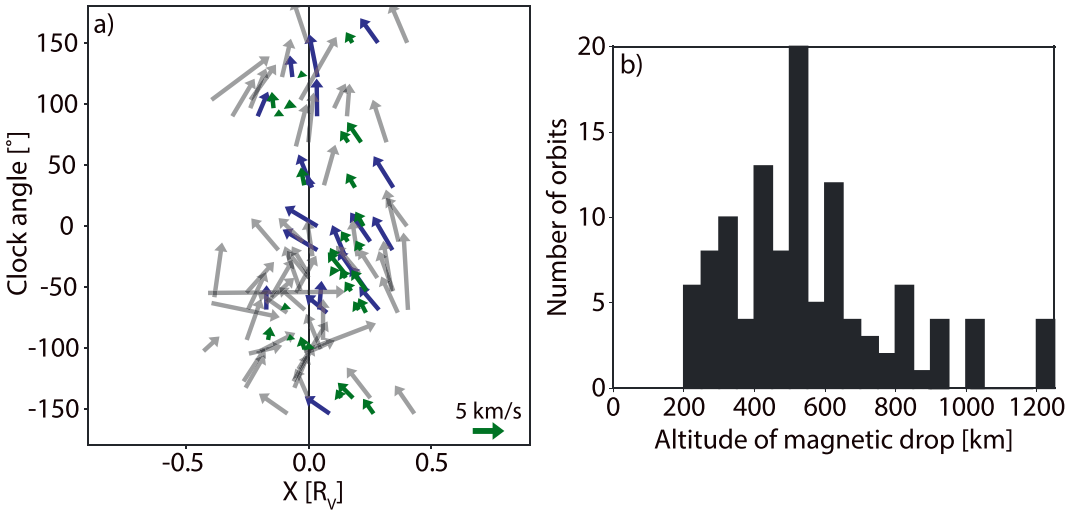

Figure 4. (a) Magnetic field effect on ion flows. Heavy ion velocity vectors are plotted against the VSO *X* and IMF clock angle field, where the clock angle could be determined. The velocity vector is the V_x-V_y components (same as Figure 3a). The colors indicate the altitude ranges: identical to Figure 3a. (b) A histogram of the altitude where the magnetic field strength drops significantly, for the same time period as the heavy ion velocity vectors, but only for the unmagnetized ionosphere cases.

$$H_p = \frac{kT}{\mu g}, \tag{1}$$

where k is the Boltzmann's constant, μ is the mean molecular mass, and g is the gravity constant. For Venus, diffusion dominates in the altitudes above ~180 km (Bauer et al., 1979), while below this altitude photochemical processes starts to dominate. The approximate ion temperature may be calculated from the scale heights at 150 and 300 km as ~490 and ~3,100 K, respectively. Although these temperatures are not fully physical, they give an indication of the plasma temperature, which are slightly higher than the temperatures measured by PVO near the equatorial terminator, 200 K at 150 km and 1,000 K at 300 km (Miller et al., 1984).

Figure 3 shows the heavy ion velocity vectors projected on (a) the *X*-*Y* plane and (b) the *X*-*R* plane ($R = \sqrt{Y^2+Z^2}$). The Venus Solar Orbital (VSO) frame is used, where *X* points toward the Sun, *Y* in the antiorbital direction of Venus around the Sun, and *Z* completes the system. Here, we again separated the nominal measurements (O^+, blue) from the pericenter measurements ($O_2{}^+$, green). The direction of the heavy ion flow in the 130–600-km altitude range in the terminator region is dusk-to-dawn (Figure 3a). The flow pattern is consistent with those of energetic neutral atom and heavy ions measured above 250 km, previously investigated by Lundin et al. (2014). In addition, Figure 3b demonstrates that the ions generally have a downward motion. The measured flow speeds show a general increase with altitude from ~2 km/s at 130 km up to ~10 km/s at 400-km altitude. These speeds are similar to or slightly higher than the speeds found at the equatorial terminator by PVO (Knudsen et al., 1980).

To constrain the effect of the magnetic field on the measurements, the data were separated according to the IMF clock angle. The clock angle is defined as arctan (B_y/B_z), where B_y and B_z are the y and z components of the IMF in the VSO frame. The clock angle was calculated from the magnetic measurements when the spacecraft was in the solar wind, that is, an average of 20 min of measurements as it approached Venus on the inbound orbit while still outside the bow shock and on the outbound orbit after the spacecraft crossed the bow shock. We only used the data when the IMF is rather stable by excluding the data under the variable IMF when the standard deviation of the 20-min measurements was more than 45° or when the angles differed more than 60° between inbound and outbound orbit segments. In Figure 4a, the heavy ion velocity vectors (V_x and V_y) are shown in the VSO X versus clock angle representation. There is no clear correlation between the flow characteristics and the clock angle.

We also investigate the influence of the ionospheric magnetization state to the flow pattern. The magnetization state of the ionosphere during the measurement time period was found to be mostly unmagnetized (~63%). Clear magnetization was found only in 11% of the orbits, and the remaining 25% were hard to distinguish due to the weak and variable magnetic field. Figure 4b shows a histogram of the ionopause altitude, when the ionosphere was unmagnetized. It is defined as where the magnetic field significantly changes (e.g., see Russell & Vaisberg, 1983, Figure 12). This altitude can only be defined for the unmagnetized state, as the magnetized state is defined as when no clear drop in the magnetic field is present. The results show that the main peak of the magnetic field drops occurs at ~300–600 km, and that the field does not penetrate below this altitude range. This is consistent with previous results of the unmagnetized Venusian ionosphere, where the IMF does not diffuse into the ionosphere as the thermal pressure of the ionosphere itself is capable of maintaining the pressure balance at the ionopause in the North Pole region. When the ionosphere is unmagnetized, the large-scale magnetic fields generally does not penetrate below 300 km (Luhmann & Cravens, 1991).

4. Interpretation

In the previous section, we showed the following characteristics of heavy ions in the ionosphere from the IMA measurements during the VEx's aerobraking campaign: (a) prominent dusk-to-dawn flow in the polar terminator region, (b) speeds increasing from ~2 km/s at 130-km altitude to >10 km/s above 400 km, and (c) a downward flow at <400-km altitude. Since the heavy ions are born in the ionosphere with almost zero speed, they should be accelerated to above 10 km/s. The accelerating forces may be driven by electromagnetic forces, momentum transfer from the solar wind, or a thermal pressure gradient. Contrary to the acceleration, a substantial drag force should be present, as the speed of the neutral atmosphere is less than the plasma speed in the measured altitude region, which is close to the exobase where the ion-neutral collisions are important. In order to understand the ion-neutral coupling in the Venusian upper ionosphere these characteristics should be explained coherently.

The electromagnetic force can accelerate the plasma in the ionosphere. This has been observed as a dominant process for the ionospheric flow on Mars (Cravens et al., 2017). However, the direction of the IMF (and resulting draped magnetic field) does not show a strong influence on the general flow pattern in the Venusian ionosphere. The general flow pattern does not show any correlations with respect to the clock angle (Figure 4a). Further, the ionosphere was mostly unmagnetized (~63%) and the altitude down to which the strong magnetic fields penetrates is ~400 km (Figure 4b). Therefore, the external electromagnetic forcing of the Venusian ionosphere, resulting from the interaction with the IMF, is expectedly not significant in this region of Venus. There might be influences of the small-scale magnetic field features in the ionosphere, which have not been measured by the magnetometer. Therefore, the acceleration by external electromagnetic forces could be less important.

Another possible acceleration mechanism is momentum transfer from the solar wind to the ionosphere (Lundin et al., 2011). Lundin et al. (2014) claim that momentum transfer is significant from their altitude profiles of the fluxes. However, the influence of the solar wind should be small in the lower altitude (<400 km) due to the very low fluxes. In addition, the nonclock angle dependence of the measurements (Figure 4a) does not favor the momentum transfer interpretation in the lower ionosphere, because momentum transfer is effective in the magnetic poles (corresponding to the clock angles of 0° and 180°; Perez-de-Tejada, 1980, 2001). On the other hand, high-speed ions seen in the higher-altitude (>500 km) dayside ionosphere with clock angle ~0° could be due to the solar wind momentum transfer.

Instead of the above two mechanisms, the third mechanism, a thermal pressure gradient force, would better explains the key observed features of the ion flow coherently. Figure 5 illustrates our interpretation of the ion flow and expected pressure gradients. Results from both PVO and this study have been included. PVO made measurements of density and temperature variations across the equatorial terminator (Taylor et al., 1980). From these results, Knudsen et al. (1981) concluded that the pressure gradient is the major force that accelerates the ions from the dayside toward the nightside (arrows 1 and 2 in Figure 5). A flow from subsolar region to the polar regions may also exist (not observed).

In a similar way, a pressure gradient between the equatorial terminator (duskside) and the pole can be formed, introducing the measured flow in this study (3, 4).

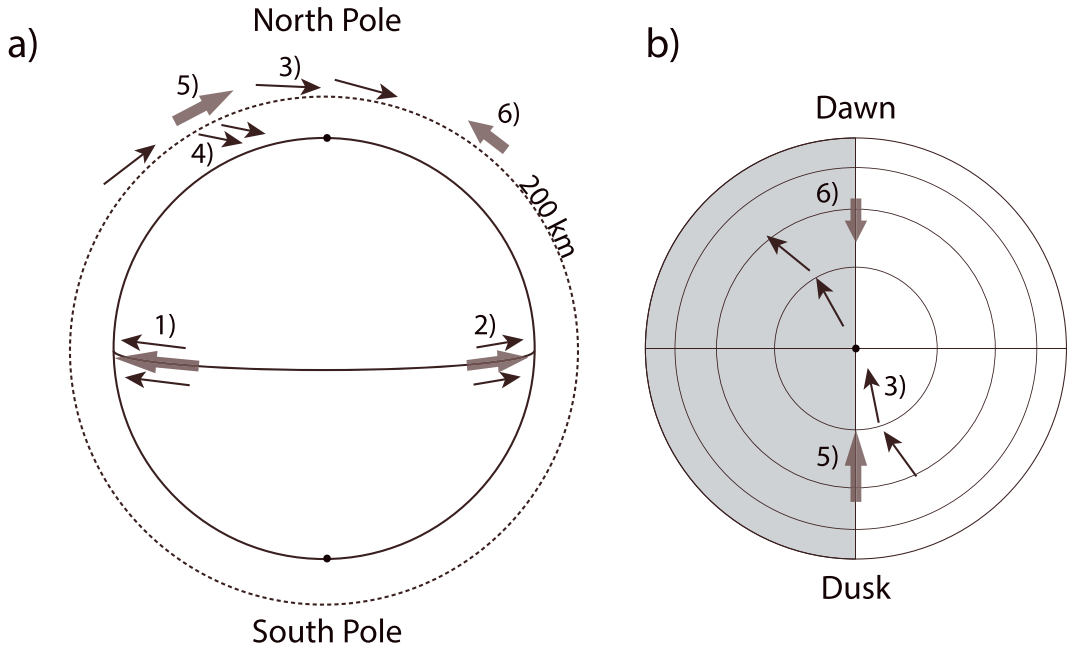

Figure 5. Schematic illustration of the ion flow pattern in the Venus ionosphere from measurements by VEx and PVO (thin arrows) as well as the expected pressure gradient forces (thick arrows). Venus is shown from (a) the dayside and (b) the north. The nightside is marked with a darker shadow. The numbering of regions is used in the explanations in the text.

As the calculated temperature from the plasma scale height (equation (1)) is very close to the measured temperatures in the equatorial region, the pressure gradient should arise from the difference in the density

$$\nabla \boldsymbol{p} = \boldsymbol{kT}\nabla \boldsymbol{n}, \tag{2}$$

where $\boldsymbol{n}$ is the density, $\boldsymbol{k}$ is the Boltzmann's constant, and $\boldsymbol{T}$ is the temperature. Due to the energy resolution of the instrument for the low-energy ions it is not straightforward to constrain the density from the IMA measurements inside the ionosphere. Instead the plasma density can be inferred from the neutral density.

The neutral density and temperature in the equatorial region is described in the VTS-3 model (Hedin et al., 1983), while in the polar region they were measured by VEx (Limaye et al., 2017). These results show that the neutral density in the polar region is about 1 order of magnitude lower than the equatorial terminator region. Considering that ionospheric ions are created mainly through photoionization in the sunlit regions of the atmosphere, in which the ion and neutral composition was observed to not significantly depend on SZA and latitude in the dayside (Fox, 2007; Hedin et al., 1983; also supported by the same scale height profiles in the polar and equatorial terminators in Figure 2), the ionization rate for each atmospheric neutral is only controlled by the solar flux. Therefore, the ion densities would also be lower in the polar region than in the equatorial terminator region.

When the pressure difference is formed between the polar and equatorial terminator regions, a thermal pressure gradient will be formed from the dusk terminator region toward the North Pole (5). In addition, a pressure gradient between the dawn terminator region and the North Pole (6) with the resulting flow toward the North Pole should exist. This has not yet been identified due to the coverage of the measurements. Most of our observations are on the duskside of the pole, with no low-altitude measurements on the dawnside of the pole. On the other hand, the neutral density on the dawnside was found to be lower than the density on the duskside (Miller et al., 1984), which would lead to a pressure gradient that is weaker on the dawnside than on duskside. Therefore, we expect an asymmetry in the pressure gradients over the pole, so that the flow would be more accelerated from the duskside over the pole and dominate in the near polar region, also on the dawnside of the pole.

Further, ions which travel along the terminator from the equator toward the pole above the exobase should continue to be accelerated, and due to the low collision rate (3), they reach the observed velocities of 10 km/s

close to the pole. A fraction of ions with downward radial velocity component can reach below the exobase (4). They will traverse the exobase far down into the collisional domain before being absorbed by the neutrals. In the collisional region of the pole, upward flux will not be seen. This is probably because the ions cannot be accelerated enough due to the high collision rate with neutrals. Such downward flux of oxygen ions was also seen in the equatorial ionosphere (Knudsen et al., 1980). The downward ion flow implies that the accelerated ions will transfer their momentum to the neutral atmosphere via the significant drag force, driving a downward flux of the neutral atmosphere. However, such a flow has not been observed. Physics of the ionosphere-thermosphere coupling and their effects on the entire Venusian system is one direction for future studies.

5. Summary

From the VEx ASPERA-4/IMA measurements, we calculated the density and velocity of the ions in the North Pole ionosphere. Currently, we only have **in situ** measurements in the North Pole region. Our results show that the accelerated ion distribution had scale heights similar to those observed during the PVO period, even though the measurement locations were slightly different. The ion flow across the polar region was found, showing a strong dusk-to-dawn directional flow along the terminator. The measurements showed ion flow speeds of 2–10 km/s, extending down into the collisional domain below the exobase, with a general decrease with altitude.

We suggest that such flow patterns in the Venusian ionosphere can be explained by a thermal pressure gradient between the equatorial terminator region and the polar region, induced by the decrease in density from the equator toward the pole. Due to the low collision rate the ions may accelerate significantly, reaching the high velocities observed. In the vicinity of the exobase, the collision rate increases and the neutral drag decreases the velocity. The interplanetary magnetic field direction has a very limited influence on the ion velocities, indicating that the external solar wind forcing is not significantly affecting the ion flow pattern inside the upper ionosphere of Venus. Rather, a thermal pressure gradient between the polar and equatorial region is capable of explaining the ion acceleration and dynamics in the Venusian ionosphere. This is in contrast with Mars, where the magnetic pressure force has the largest effect on the ion motion in the Martian ionosphere.

Acknowledgments
The Swedish contribution to the ASPERA-4 experiment on board Venus Express was supported by the Swedish National Space Agency (SNSA). We acknowledge the European Space Agency (ESA) for supporting the successful Venus Express mission, with particular efforts of the operation during the aerobraking phase. M. Persson acknowledges support of her graduate studies from SNSA (Dnr: 129/14). ASPERA-4/IMA and MAG data used in this study are publicly available via the ESA Planetary Science Archive at https://www.cosmos.esa.int/web/psa/venus-express.

References

Angsmann, A., Fränz, M., Dubinin, E., Woch, J., Barabash, S., Zhang, T. L., & Motschmann, U. (2011). Magnetic states of the ionosphere of Venus observed by Venus Express. *Planetary and Space Science*, *59*(4), 327–337. https://doi.org/10.1016/j.pss.2010.12.004

Barabash, S., Sauvaud, J. A., Gunell, H., Andersson, H., Grigoriev, A., Brinkfeldt, K., et al. (2007). The Analyser of Space Plasmas and Energetic Atoms (ASPERA-4) for the Venus Express mission. *Planetary and Space Science*, *55*(12), 1772–1792. https://doi.org/10.1016/j.pss.2007.01.014

Bauer, S. J., Donahue, T. M., Hartle, R. E., & Taylor, H. A. (1979). Venus ionosphere: Photochemical and thermal diffusion control of ion composition. *Science*, *205*(4401), 109–112. https://doi.org/10.1126/science.205.4401.109

Bougher, S. W., Rafkin, S., & Drossart, P. (2006). Dynamics of the Venus upper atmosphere: Outstanding problems and new constraints expected from Venus Express. *Planetary and Space Science*, *54*(13-14), 1371–1380. https://doi.org/10.1016/j.pss.2006.04.023

Butler, D. M., & Chamberlain, J. W. (1976). Venus' night side ionosphere: Its origin and maintenance. *Journal of Geophysical Research*, *81*(25), 4757–4760. https://doi.org/10.1029/JA081i025p04757

Carlsson, E., Fedorov, A., Barabash, S., Budnik, E., Grigoriev, A., Gunell, H., & Dierker, C. (2006). Mass composition of the escaping plasma at Mars. *Icarus*, *182*(2), 320–328. https://doi.org/10.1016/j.icarus.2005.09.020

Colin, L. (1980). The Pioneer Venus program. *Journal of Geophysical Research*, *85*(A13), 7575–7598. https://doi.org/10.1029/JA085iA13p07575

Cravens, T. E., Hamil, O., Houston, S., Bougher, S., Ma, Y., Brain, D., & Ledvina, S. (2017). Estimates of ionospheric transport and ion loss at Mars. *Journal of Geophysical Research: Space Physics*, *122*, 10,626–10,637. https://doi.org/10.1002/2017JA024582

Dubinin, E., Fraenz, M., Zhang, T. L., Woch, J., & Wei, Y. (2014). Magnetic fields in the Venus ionosphere: Dependence on the IMF direction: Venus Express observations. *Journal of Geophysical Research: Space Physics*, *119*, 7587–7600. https://doi.org/10.1002/2014JA020195

Fox, J. L. (2007). Near-terminator Venus ionosphere: How chapman-esque? *Journal of Geophysical Research*, *112*, E04S02. https://doi.org/10.1029/2006JE002736

Fox, J. L., & Sung, K. Y. (2001). Solar activity variations of the Venus thermosphere/ionosphere. *Journal of Geophysical Research*, *106*(A10), 21,305–21,335. https://doi.org/10.1029/2001JA000069

Fränz, M., Dubinin, E., Roussos, E., Woch, J., Winningham, J. D., Frahm, R., et al. (2006). Plasma moments in the environment of Mars. *Space Science Reviews*, *126*(1-4), 165–207. https://doi.org/10.1007/s11214-006-9115-9

Futaana, Y., Stenberg Wieser, G., Barabash, S., & Luhmann, J. (2017). Solar wind interaction and impact on the Venus atmosphere. *Space Science Reviews*, *212*(3-4), 1453–1509. https://doi.org/10.1007/s11214-017-0362-8

Hedin, A. E., Niemann, H. B., Kasprzak, W. T., & Seiff, A. (1983). Global empirical model of the Venus thermosphere. *Journal of Geophysical Research*, *88*(A1), 73–83. https://doi.org/10.1029/JA088iA01p00073

Knudsen, W. C., Spenner, K., & Miller, K. L. (1981). Anti-solar acceleration of ionospheric plasma across the Venus terminator. *Geophysical Research Letters*, *8*(3), 241–244. https://doi.org/10.1029/GL008i003p00241

Knudsen, W. C., Spenner, K., Miller, K. L., & Novak, V. (1980). Transport of ionospheric O^+ ions across the Venus terminator and implications. *Journal of Geophysical Research*, *85*(A13), 7803–7810. https://doi.org/10.1029/JA085iA13p07803

Knudsen, W. C., Spenner, K., Whitten, R. C., Spreiter, J. R., Miller, K. L., & Novak, V. (1979). Thermal structure and major ion composition of the Venus ionosphere: First RPA results from Venus Orbiter. *Science*, *203*(4382), 757–763. https://doi.org/10.1126/science.203.4382.757

Limaye, S. S., Lebonnois, S., Mahieux, A., Pätzold, M., Bougher, S., Bruinsma, S., et al. (2017). The thermal structure of the Venus atmosphere: Intercomparison of Venus Express and ground based observations of vertical temperature and density profiles. *Icarus*, *294*(15), 124–155. https://doi.org/10.1016/j.icarus.2017.04.020

Luhmann, J., & Cravens, T. E. (1991). Magnetic fields in the ionosphere of Venus. *Space Science Reviews*, *55*(1-4), 201–274. https://doi.org/10.1007/BF00177138

Lundin, R., Barabash, S., Futaana, Y., Holmström, M., Sauvaud, J. A., & Fedorov, A. (2014). Solar wind-driven thermospheric winds over the Venus north polar region. *Geophysical Research Letters*, *41*, 4413–4419. https://doi.org/10.1002/2014GL060605

Lundin, R., Barabash, S., Futaana, Y., Sauvaud, J. A., Fedorov, A., & Perez-de-Tejada, H. (2011). Ion flow and momentum transfer in the Venus plasma environment. *Icarus*, *215*(2), 751–758. https://doi.org/10.1016/j.icarus.2011.06.034

Mariner Stanford Group (1967). Venus: Ionosphere and atmosphere as measured by dual-frequency radio occultation of Mariner V. *Science*, *158*(3809), 1678–1683. https://doi.org/10.1126/science.158.3809.1678

Miller, K. L., & Knudsen, W. C. (1987). Spatial and temporal variations of the ion velocity measured in the Venus ionosphere. *Advances in Space Research*, *7*(12), 107–110. https://doi.org/10.1016/0273-1177(87)90207-9

Miller, K. L., Knudsen, W. C., & Spenner, K. (1984). The dayside Venus ionosphere I. Pioneer Venus retarding potential analyzer experimental observations. *Icarus*, *57*(3), 386–409. https://doi.org/10.1016/0019-1035(84)90125-8

Müller-Wodarg, I. C. F., Forbes, J. M., & Keating, G. M. (2006). The thermosphere of Venus and its exploration by a Venus Express Accelerometer Experiment. *Planetary and Space Science*, *54*(13-14), 1415–1424. https://doi.org/10.1016/j.pss.2006.04.029

Perez-de-Tejada, H. (1980). Viscous flow circulation of the solar wind behind Venus. *Science*, *207*(4434), 981–983. https://doi.org/10.1126/science.207.4434.981

Perez-de-Tejada, H. (2001). Solar wind erosion of the Venus polar ionosphere. *Journal of Geophysical Research*, *106*(A1), 211–219. https://doi.org/10.1029/1999JA000231

Perez-de-Tejada, H., Reyez-Ruiz, M., & Durand-Manterola, H. (2010). Viscous flow properties in the transport of solar wind momentum to the Venus upper ionosphere. *Icarus*, *206*(1), 182–188. https://doi.org/10.1016/j.icarus.2009.05.023

Russell, C. T., & Vaisberg, O. (1983). The interaction of the solar wind with Venus. In D. M. Hunten, L. Colin, T. M. Donahue, & V. I. Moroz (Eds.), *Venus*, (p. 873). Tucson: Univ. of Arizona Press.

Svedhem, H., Titov, D. V., McCoy, D., Lebreton, J.-P., Barabash, S., Bertaux, J.-L., et al. (2007). Venus Express—The first European mission to Venus. *Planetary and Space Science*, *55*(12), 1636–1652. https://doi.org/10.1016/j.pss.2007.01.013

Taylor, H. A. Jr., Brinton, H. C., Bauer, S. J., Hartle, R. E., Cloutier, P. A., & Daniell, R. E. Jr. (1980). Global observations of the composition and dynamics of the ionosphere of Venus: Implications for the solar wind interaction. *Journal of Geophysical Research*, *85*(A13), 7765–7777. https://doi.org/10.1029/JA085iA13p07765

Taylor, H. A. Jr., Brinton, H. C., Bauer, S. J., Hartle, R. E., Cloutier, P. A., Daniell, R. E. Jr., & Donahue, T. M. (1979). Ionosphere of Venus: First observations of day-night variations of the ion composition. *Science*, *205*(4401), 96–99. https://doi.org/10.1126/science.205.4401.96

Zhang, T., Delva, M., Baumjohann, W., Volwerk, M., Russell, C., Barabash, S., et al. (2008). Initial Venus Express magnetic field observations of the magnetic barrier at solar minimum. *Planetary and Space Science*, *56*(6), 790–795. Mars Express/Venus Express. https://doi.org/10.1016/j.pss.2007.10.013

Zhang, T. L., Baumjohann, W., Russell, C. T., Luhmann, J. G., & Xiao, S. D. (2016). Weak, quiet magnetic fields seen in the Venus atmosphere. *Nature Scientific Reports*, *6*(1), 23537. https://doi.org/10.1038/srep23537

Zhang, T. L, BergHofer, G., Magnes, W., Delva, M., Baumjohann, W., Biernat, H., et al. (2007). MAG: The fluxgate magnetometer of Venus Express. ESA Special Publication, SP 1295:1–10.

References From the Supporting Information

Bergman, S., G. Stenberg Wieser, M. Wieser, and F. Johansson (2018). Correction of low-energy ion measurements from Rosetta-ICA for the effects of spacecraft charging. Abstract presented at EPSC, Berlin, Germany. Vol. 12, EPSC2018-230.

Garrett, H. B. (1981). The charging of spacecraft surfaces. *Reviews of Geophysics and Space Physics*, *19*(4), 577–616. https://doi.org/10.1029/RG019i004p00577